

# Temperature Inversion in the Io Plasma Torus

NICOLE MEYER-VERNET, MICHEL MONCUQUET, AND SANG HOANG

*Département de Recherche Spatiale, CNRS URA 264, Observatoire de Paris, 92195 Meudon, Cedex, France*

E-mail: meyer@obspm.fr

Received September 27, 1994; revised January 19, 1995

We present *in situ* measurements of electron parameters as a function of latitude in the Io plasma torus, deduced from an extended analysis of the radio and plasma wave data acquired on board Ulysses. We find that the density and temperature are anticorrelated and obey an approximate polytrope law  $T_e \propto 1/\sqrt{n_e}$ . We interpret this result with a simple model based on velocity filtration by the potential which confines the particles to the equator. In the absence of local thermal equilibrium, suprathermal particles overcome more easily the potential; thus the temperature increases with latitude in anticorrelation with the density, which decreases less steeply than the Gaussian corresponding to equilibrium. This explains the observed polytrope relation, and the calculated densities fit quite well the measured density profile. These results illustrate in the Io torus a general behavior of low-density inhomogeneous plasmas, anticipated by J. D. Scudder (1992, *Astrophys. J.* 398, 299–319). © 1995 Academic Press, Inc.

## 1. INTRODUCTION

In February 1992, the Ulysses spacecraft passed through the Io plasma torus. A preliminary estimate of electron density and temperature was obtained by Hoang *et al.* (1993) from the spectrum of the plasma quasi-thermal noise (Meyer-Vernet and Perche 1989) measured by the radio and plasma wave experiment (Stone *et al.* 1992a). This determination used both the upper-hybrid frequency peak, as in (Stone *et al.* 1992b), and a novel technique based on the polarization of Bernstein waves (Meyer-Vernet *et al.* 1993). A detailed analysis of the data has subsequently given the dispersion characteristics of these waves (Moncuquet *et al.* 1995), yielding more precise and extended results. The present paper studies these *in situ* values of the electron density and temperature as a function of latitude in the torus.

The Ulysses trajectory was basically north-to-south (crossing the jovian magnetic equator at about  $8R_J$  from Jupiter), in contrast to Voyager which explored the torus near the equatorial plane. Hence the present results provide the first *in situ* measurement of the torus latitudinal structure; they are unique, since Ulysses particle analyzers were not operating near Jupiter. This may be an

important key to understanding this medium, of which no self-consistent theory yet exists, and whose energy balance is not fully understood (see for example Barbosa *et al.* 1983, Smith and Strobel 1985, Smith *et al.* 1988, Strobel 1989).

We first briefly recall the principle of the measurement and its significance when the plasma is not in equilibrium. We then show that, instead of being constant along magnetic field lines—as currently assumed in the torus models (Bagenal and Sullivan 1981, Divine and Garrett 1983, Bagenal 1994)—the (bulk) temperature varies with latitude in anticorrelation with the density, following an approximate polytrope law with an exponent smaller than one.

We suggest a simple interpretation in terms of velocity filtration by the ambipolar electric field set up in the presence of plasma corotation, which tends to confine particles close to the centrifugal equator: since the more energetic electrons overcome more easily the confining potential, their proportion increases outside the equatorial region, whereas the bulk density decreases; so the density and temperature are anticorrelated. This mechanism works only if the velocity distribution is not Maxwellian. This basic property of a confining potential to act as a high-pass filter for particle energies—yielding anticorrelated density and temperature—was first noted by Scudder (1992a), who suggested that it should hold in many astrophysical contexts and used it to explain temperature inversions in stellar coronae (Scudder 1992b). This allows us to build a simple model of the latitudinal density profile in the outer plasma torus, which we will compare with our observations.

## 2. ELECTRON MEASUREMENTS FROM BERNSTEIN WAVES

### 2.1 Electron Density and Temperature

Measurements of the dispersion characteristics of electrostatic waves reveal the properties of the ambient plasma electrons. In the Io torus, the Ulysses filamental dipole antennae were longer than electrostatic wavelengths; in this case, the antenna's directivity pattern is

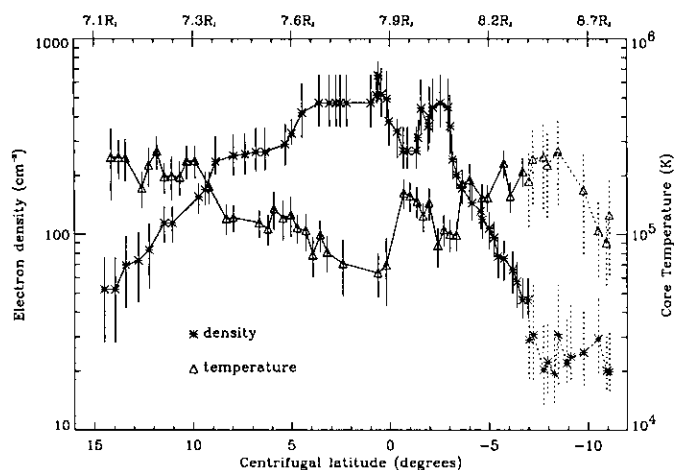


FIG. 1. Electron density and temperature versus jovian centrifugal latitude, measured *in situ* by the radio and plasma wave experiment aboard Ulysses. The corresponding joviocentric distance in jovian radii is indicated at the top. (Dotted error bars identify the data for which the measurements of  $n_e$  and  $T_e$  are not independent of each other.)

especially suitable for deducing the electrostatic wave vector modulus  $k$  from the observed polarization (Meyer-Vernet 1994). This method has been extensively applied to the plasma quasi-thermal noise measured aboard Ulysses between the electron gyroharmonic frequencies to deduce dispersion characteristics  $k(\omega)$  of Bernstein waves in the Io torus (Moncuquet *et al.* 1995).

If the electrons are Maxwellian, with temperature  $T_e$ , the normalized dispersion relation  $\sqrt{T_e} \times k(\omega)$  is known theoretically (Bernstein 1958) and depends only on the magnetic field  $B$  and the plasma frequency  $f_p$ . Using independent measurements of  $B$  from the inboard magnetometer (Balogh *et al.* 1992) or from the wave spectral minima (Meyer-Vernet *et al.* 1993), and of  $f_p$  (Hoang *et al.* 1993), one can thus deduce the temperature  $T_e$  by fitting the theoretical dispersion curves to the experimental ones (Moncuquet *et al.* 1995). Since  $T_e$  is the sole unknown parameter in the fitting, this determination can be fairly precise. If the electrons are not Maxwellian, this method gives an effective temperature which is defined in Section 2.2.

The temperature thus obtained is plotted in Fig. 1 from +15 to  $-7^\circ$  jovian centrifugal latitude (the latitude is referenced to the classical centrifugal surface reference, using an approximate tilted dipole magnetic field model). We have superimposed the density  $n_e = (f_p/9)^2$  (in S.I. units) determined by Hoang *et al.* (1993). It is important to note that in this region, our measurements of  $T_e$  are based on a part of the dispersion relation which is nearly independent of  $f_p$  (because  $f_p$  is large enough); thus any correlation observed between  $n_e$  and  $T_e$  cannot be an artifact due to the measuring process.

For negative latitudes beyond  $-7^\circ$  in the torus, no independent measurement of  $f_p$  could be obtained. In that region, Moncuquet *et al.* (1995) deduced both  $n_e$  and  $T_e$ , by using the full-dispersion characteristics. These measurements of  $n_e$  and  $T_e$  are thus not independent and are less precise. They are plotted in Fig. 1 with dotted error bars and will not be used in analyzing the relation between  $n_e$  and  $T_e$ .

## 2.2. Significance of the Temperature

It is important to discuss the significance of the measured temperature, since the electron velocity distribution is not Maxwellian in the region explored. The electron analyzers aboard Voyager (Scudder *et al.* 1981, Sittler and Strobel 1987) detected at this joviocentric distance  $R \approx 8R_J$  a suprathermal population 10–30 times hotter than the main (cold) population and representing a few percent of the total density. The presence of such a population was confirmed by Ulysses data, since it allowed us to interpret quantitatively the suprathermal level of electrostatic fluctuations in Bernstein waves (Meyer-Vernet *et al.* 1993). This minor hot population does not affect significantly the part of the dispersion relation used in our temperature measurements (Moncuquet *et al.* 1995), so that, if the velocity distribution were a mere superposition of a cold and such a hot population, both being Maxwellian, the measured temperature plotted in Fig. 1 would be approximately that of the main (cold) population.

However, the velocity distribution is expected to be more complex than a superposition of two Maxwellians. First, the Voyager electron analyzer results clearly showed that the hot electrons were not Maxwellian distributed (Scudder *et al.* 1981). Second, these analyzers had a low-energy threshold of 10 eV, and the spacecraft was negatively charged, thereby yielding a higher effective threshold (Scudder *et al.* 1981, Sittler and Strobel 1987); since  $10 \text{ eV} \approx 1.2 \times 10^5 \text{ K}$  in temperature units, this implies that a significant part of the main (cold) population could not be detected, so that the precise shape of the distribution at low energies is unknown. Hence, although the cold electron distribution could be roughly fitted to a Maxwellian, it is not certain that it was precisely Maxwellian. On the other hand, aboard Ulysses, the particle analyzers were unfortunately not operating in the torus, and the frequency range in which we measured the dispersion relation was not large enough to settle that question.

Hence, let us consider a more general case: a non-Maxwellian distribution made of a superposition of several Maxwellians of densities  $n_\alpha$  and temperatures  $T_\alpha$ . Since our Bernstein wave measurements were mostly made in the middle of the first gyroharmonic band, it can be shown (Moncuquet *et al.* 1995) that they are not

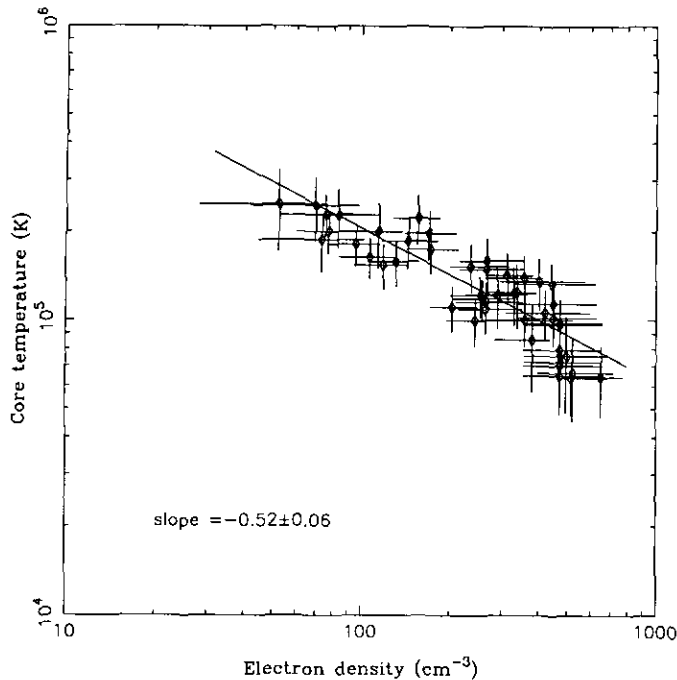


FIG. 2. Electron parameters measured *in situ* aboard Ulysses, plotted as temperature versus density, and the associated best-fit line. The data span  $\sim 3R_J$  in latitudinal distance. (The longitude varies by  $\approx 90^\circ$ , centered near  $\lambda_{\text{CML}} \approx 310^\circ$ , and the joviocentric distance varies only from 7.1 to 8.4  $R_J$ . We have used the data plotted with solid error bars in Fig. 1, which are independent measurements of  $n_e$  and  $T_e$ .)

sensitive to the mean energy of the distribution, i.e., to the traditional temperature  $T = \sum n_\alpha T_\alpha / \sum n_\alpha$ . Instead, our measurements give an effective temperature  $T_{\text{eff}}$  defined by

$$1/T_{\text{eff}} = \sum_\alpha (n_\alpha / T_\alpha) / \sum_\alpha n_\alpha$$

if the densities and temperatures of the individual populations have similar orders of magnitude or if the hot population densities are much smaller than that of the coldest one. In this case, the temperature plotted here is thus  $T_{\text{eff}}$ . This effective temperature  $T_{\text{eff}}$  is defined from the mean *inverse* energy of the particles and is thus mainly sensitive to the cold electrons; this is reminiscent of the classical Debye shielding, which depends on the same effective temperature, albeit for different reasons (Meyer-Vernet 1993).

### 3. POLYTROPE RELATION

#### 3.1. Relation between Density and Temperature

Let us study the relation between  $n_e$  and  $T_e$ . We only consider the region from  $+15$  to  $-7^\circ$  centrifugal latitude, where the  $n_e$  and  $T_e$  measurements are independent and the uncertainties rather small. Figure 2 shows the data

plotted as temperature versus density in a log-log format and the associated best-fit line. Since it would be inadequate to determine the slope from a classical linear least-squares fitting, because of the finite errors bars on both  $n_e$  and  $T_e$ , we used a standard (nonlinear) approach taking into account the uncertainties on both variables (Press *et al.* 1992); to calculate the  $\chi^2$  merit function, the square deviations between measurements and model are weighted by  $1/(\sigma_{T_e}^2 + (\gamma - 1)^2 \sigma_{n_e}^2)$ , where  $\sigma_{T_e}$  and  $\sigma_{n_e}$  are the measurement uncertainties and  $\gamma - 1$  the slope to be determined, in log-log coordinates. This yields the polytrope relation

$$T_e \propto n_e^{\gamma-1}, \quad (2)$$

with  $\gamma = 0.48 \pm 0.06$  ( $3\sigma$ ).

The correlation coefficient between  $n_e$  and  $T_e$  is  $r = -0.87$ . Given the number of data points (46), the level of significance of that anticorrelation is very high.

#### 3.2. Discussion

Some anticorrelation between  $n_e$  and  $T_e$  can also be seen in some of the results of the particle analyzers aboard Voyager, although it has not been quantified (Scudder *et al.* 1981, Sittler and Strobel 1987). However, as we said, Voyager mainly explored the variations with joviocentric distance near the equator, whereas Ulysses mainly explored the variation with latitude. Indeed, the region involved in Fig. 2 spans  $\sim 3R_J$  in full latitudinal extension but only  $\sim 1R_J$  in joviocentric distance. Owing to that special trajectory and to the general predominance of the latitudinal gradient over the radial one, most of the variation observed here in  $n_e$  and  $T_e$  can be ascribed to the change in latitude. This is confirmed by the approximate latitudinal symmetry exhibited in Fig. 1 (whereas the small variation in joviocentric distance should be responsible for most of the slight asymmetry observed; we will return to this point in Section 5.3.).

The presence of the jovian magnetic field—with the corresponding very small particle gyroradii—makes the physics of the latitudinal and radial variations basically different, since they take place, respectively, along and across  $\mathbf{B}$ . With the largest density and smallest temperature measured here in the vicinity of equator (i.e.,  $n_e \approx 650 \text{ cm}^{-3}$  with  $T_e \approx 6.3 \times 10^4 \text{ K}$ ), the free path of thermal electrons for Coulomb collisions with like particles (Spitzer 1962) is  $l_{\text{pm}} \approx 6R_J$ . Since  $l_{\text{pm}} \propto T_e^2/n$ , the mean free path is larger away from the equator, and still larger for suprathermal electrons. Other free paths, such as those corresponding to Coulomb encounters with ions and/or with the hot electron population—or to collisional ionization or excitation, or recombination—are of the same order or larger, as are ion-free paths (see Strobel

1989). On the other hand, one sees in Fig. 1 that  $T_e$  typically increases by a factor of two—whereas  $n_e$  decreases by a factor of four—over about  $7^\circ$  latitude, which corresponds to a distance of only  $\sim 1R_J$  along field lines. This is much smaller than the free paths estimated above. Thus the time for a particle to move over a characteristic scale length along  $\mathbf{B}$  is short compared to other time scales. The reverse is true in the radial direction, since the time scales for diffusion perpendicular to  $\mathbf{B}$  are expected to be very large (see for example Siscoe and Summers 1981).

The polytrope relation  $T_e \propto 1/\sqrt{n_e}$  found here over more than one decade in density is incompatible with the assumption of constant (bulk) temperature along field lines made in the torus models (see Divine and Garrett 1983, Bagenal and Sullivan 1981, Bagenal 1994), since, as we said, our measured temperature is mostly sensitive to the bulk cold electron population. It would also be difficult to explain our results by longitudinal asymmetries (Desch *et al.* 1994), since such an explanation would require an ad hoc fourfold temperature variation over  $\sim 45^\circ$  longitude, being, by chance, adequately symmetrical.

Our results are also incompatible with an adiabatic ( $\gamma = 5/3$ ), or CGL (Chew *et al.* 1956) double-adiabatic behavior. In particular, with an anisotropic distribution, our measurement gives the temperature  $T_{e\perp}$  perpendicular to  $\mathbf{B}$  (Meyer-Vernet *et al.* 1993), and the results are then incompatible with the CGL relation  $T_{e\perp} \propto B$ , since  $B$  varies by less than 15% over  $10^\circ$  latitude. This is not surprising since with free paths so large as compared to the scale height, the traditional fluid closure approximations are not expected to be applicable; the existence of important parallel electric fields strongly violates the CGL ordering scheme further (anyway, one would not expect to find an adiabatic or double-adiabatic behavior along field lines, since they are perpendicular to the mean bulk velocity, so the fluid energy equation has no component parallel to  $\mathbf{B}$ ).

With these large free paths, one should use a microscopic plasma description, i.e., take explicitly the velocity distribution into account. In this case, it is well known that with an isotropic Maxwellian, the temperature should be constant along field lines (see Section 4.3), which is incompatible with our results. Adding a hot Maxwellian tail to the distribution (Sittler and Strobel 1987, Bagenal 1994) cannot explain our results either, since our measurement scheme is roughly insensitive to the hot component (we will return to this point in Section 4.5). Now, what would happen with an anisotropic Maxwellian, i.e., the so-called bi-Maxwellian? The problem has been formulated in detail by Chiu and Schulz (1978) and applied in particular to Jupiter by Huang and Birmingham (1992) without considering the problem of accessibility in phase space. Under that assumption, which is relevant in the latitude range considered here, the sense of anisotropy

expected in the torus ( $T_\perp \gtrsim T_\parallel$ ) should produce a *decrease* in  $T_\perp$  with latitude (Huang and Birmingham 1992). To yield a temperature increase, the sense of anisotropy should be opposite; moreover, the relative increase should then be necessarily smaller than that of  $B$ , i.e., rather small, whatever the anisotropy factor.

Hence, a microscopic plasma description cannot explain our results if the (bulk) velocity distribution is a Maxwellian or a bi-Maxwellian.

This is not surprising with the above parameters since the collisions are not expected to be sufficient to drive the distributions to local Maxwellians (or bi-Maxwellians) in the presence of the latitudinal gradient. Even if the free paths of thermal particles were not so large, the presence of the suprathermal particles—which have free access to still larger distances since the free paths increase as the fourth power of the velocity—should preclude the achievement of local thermal equilibrium. The basic importance of such a nonlocal behavior in space plasmas was first noted by Scudder and Olbert (1979) in the context of the solar wind.

## VELOCITY FILTRATION IN THE IO TORUS

### 4.1. Position of the Problem

In the outer torus, the main external force acting on the charged particles along the magnetic field is produced by the centrifugal force due to plasma corotation. As is well known, since the electrons are much lighter than ions, they feel a much smaller centrifugal force and an ambipolar electric field must exist to preserve local charge quasi-neutrality. This field confines the electrons in the same region as ions, i.e., near the point along any given magnetic field line where the  $\mathbf{B}$ -aligned component of the centrifugal force vanishes (Gledhill 1967); this defines the so-called centrifugal equator (which is slightly shifted from the magnetic equator since the planet's magnetic and spin axes do not exactly coincide).

In a first approximation, the particles are thus confined near the equator by forces deriving from potentials: the electrostatic force for electrons, the electrostatic force plus the centrifugal one for ions. Since the main source of these particles is also near equator, the situation has some similarity with the problem considered by Scudder (1992a,b), to interpret temperature inversions in stellar coronae: basically, since the more energetic particles overcome more easily the confining potential, their proportion is larger outside the potential well, so that the mean kinetic energy of particles increases with latitude as the density falls. This does not happen with a Maxwellian distribution because, in this case, the attractive potential filtrates all particles of the distribution in the same way (it produces a translation in  $v^2$  which just multiplies  $e^{-v^2/v_e^2}$  by a constant factor).

To illustrate this velocity filtration effect, we consider a very simplified model. Since the particle free paths are much larger than the characteristic scale lengths (see Section 3.2), we treat the latitudinal variation over a few scale lengths as a collisionless problem. In the latitude range considered here and with a roughly dipolar magnetic field, the field-aligned component of the centrifugal force on ions of mass  $m_i$  may be approximated by

$$F_c \approx -3m_i \Omega_J^2 z, \quad (3)$$

$z \ll R$  being the distance along magnetic field lines (counted from the centrifugal equator), which is roughly proportional to the centrifugal latitude, and  $\Omega_J$  being the planet's spin angular frequency (see for example Siscoe (1977)). We neglect the field-aligned component of the gravitational force, which is smaller by a factor of  $2M_J G / (3 \Omega_J^2 R^3) \approx 0.015$  at the jovian distance  $R \approx 8R_J$ ,  $M_J$  being the jovian mass and  $G$  the gravitational constant. In the latitude range and with the parameters considered here, the magnetic field variations are very small over the latitudinal characteristic length of about  $1R_J$ ; hence, we will also neglect them (i.e., we neglect the magnetic mirror force).

Since, as we said, the centrifugal force on electrons is much smaller than the corresponding force  $F_c$  on ions, the charge neutrality condition requires that the electrons be subjected to an electric field confining them near  $z = 0$ , as are the ions. The corresponding electric potential may thus be taken as  $\Phi(z) < 0$ , with  $\Phi(0) = 0$  and  $d|\Phi|/dz > 0$  for  $z \ll R$ .

#### 4.2. Velocity Distribution and Generalized Temperatures

Let  $f_0(v)$  be the electron velocity distribution at  $z = 0$ , which we assume for simplicity to be isotropic. This approximation is reasonable since the bulk of the electrons has been inferred to be roughly isotropic in this region: an observation made during a Voyager roll maneuver was found to be compatible with  $T_\perp/T_\parallel \sim 1.2$  at  $10^\circ$  latitude for the bulk population (Sittler and Strobel 1987); such a small anisotropy is expected to have negligible consequences on our results.

From Liouville's theorem, the velocity distribution is constant along particle trajectories, so that the distribution at distance  $z$  is  $f(z, v) = f_0(v_0)$  with, from conservation of energy

$$m_e v^2/2 - e\Phi(z) = m_e v_0^2/2.$$

We consider only latitudes such that  $z \ll R$ , where the potential is attractive and monotonic (with  $B$  nearly constant), so that the isotropy of the velocity distribution is

preserved and the trajectories at  $z$  connect to  $z = 0$  (the problem of accessibility in phase space should be considered for higher latitudes, where the potential is not monotonic). We thus have

$$f(z, v) = f_0[\sqrt{v^2 + V^2(z)}] \quad (4)$$

with

$$V^2(z) = 2e|\Phi(z)|/m_e.$$

The moment of order  $q$  of the velocity distribution at distance  $z$  along  $\mathbf{B}$  is

$$\begin{aligned} M_q(z) &= \int d^3v v^q f(z, v) \\ &= 4\pi \int_0^\infty dv v^{2+q} f_0[\sqrt{v^2 + V^2(z)}]. \end{aligned} \quad (5)$$

The density  $n_e$  is the moment of order  $q = 0$ , i.e.,  $n_e = M_0$ . In general,  $f_0$  is a decreasing function of the velocity; as a consequence, since  $V^2 \propto |\Phi|$  increases monotonically with  $z$ ,  $f_0[\sqrt{v^2 + V^2}]$  decreases with  $z$ . Hence, all the moments  $M_q$  decrease with  $z$ ; this is true in particular of the density.

In the absence of local thermal equilibrium, the concept of "temperature" is not straightforward, and different types of measurements can give different results. So we define generalized temperatures  $T_q$  as

$$\frac{k_B T_q}{m_e} = \left[ \frac{M_q}{M_0 C_q} \right]^{2/q} \quad (\text{for } -3 < q \neq 0) \quad (6)$$

$$\text{with } C_q = |1 \times 3 \cdots (q+1)| \quad (q \text{ even}) \quad (7)$$

$$C_q = 2^{1+q/2} [(q+1)/2]! / \sqrt{\pi} \quad (q \text{ odd}). \quad (8)$$

This normalization has been chosen in such a way that all  $T_q$ s are equal to  $T_M$  if the distribution is a Maxwellian of temperature  $T_M$ ; i.e.,

$$f(v) \propto \exp(-m_e v^2/2k_B T_M). \quad (9)$$

On the other hand, for a non-Maxwellian distribution, the temperatures  $T_q$  are different. In the non-Maxwellian case, the "temperature" is traditionally defined as the mean random energy times  $2/3k_B$ , which is just our generalized temperature of order  $q = 2$ ; i.e.,  $T_2 = m_e M_2/3k_B M_0$ . This traditional definition is adequate when the physics and/or the measuring device are sensitive to the mean random energy of the particles. However, many temperature measuring techniques are sensitive instead to different moments of the distribution, i.e., to other  $T_q$ . For example, a measurement of the Debye length would give

the effective temperature  $T_{-2}$ , since  $L_D = (\epsilon_0 k_B T_{-2} / n_e e^2)^{1/2}$ ; on the other hand, a measurement of the random flux would give  $T_1$ , since the mean random velocity is  $\langle v \rangle = (8k_B T_1 / \pi m_e)^{1/2}$ .

#### 4.3. Generic Anticorrelation between Density and Generalized Temperatures

Let us first consider the classical case where  $f_0$  is a Maxwellian of temperature  $T_M$ . One sees from (4) that the distribution remains Maxwellian for  $z \neq 0$ , with the same temperature, and from (5), that all the moments  $M_q$  vary with  $z$  as  $e^{-e|\Phi|/k_B T_M}$ . This would justify the widely used assumption of constant temperatures along magnetic field lines, if the particle velocity distributions were actually Maxwellian; of course, in this case, the density and temperature are not anticorrelated.

If the distribution  $f_0$  is now a linear combination of Maxwellians, so that there is no more thermal equilibrium, the temperatures  $T_q$  are no longer equal to each other, nor independent of  $z$  (although the temperature of each Maxwellian is independent of  $z$ ). The  $T_q$  generally increase with  $q$ , since higher-order moments favor components of higher temperatures. In particular, the effective temperature given by Eq.(1) is then  $T_{\text{eff}} = T_{-2} = m_e M_0 / k_B M_{-2}$ . In the Appendix, we show analytically that with such a distribution and a monotonic potential which attracts particles to  $z = 0$ , all the generalized temperatures  $T_q$  increase with  $z$ . Hence, since the density decreases with  $z$ , all the temperatures  $T_q$  vary in anticorrelation with  $n_e$ . An important consequence is that *if a polytrope law  $T_q \propto n_e^{\gamma-1}$  does exist, its index is necessarily smaller than one* (or just equal to one in the limiting case of a Maxwellian distribution.)

This generalizes to the temperatures  $T_q$  the anticorrelation between density and temperature first shown by Scudder (1992a) in a general context, for the traditional temperature, using graphical arguments; this is a generic property of nonthermal distributions.

#### 4.4. Kappa Distribution

Instead of a superposition of a several Maxwellians, let us consider the simpler nonthermal distribution:

$$f_0(v) \propto \left[ 1 + \frac{v^2}{\kappa v_e^2} \right]^{-\kappa-1} \quad (10)$$

This generalized Lorentzian function is very convenient to model observed velocity distributions (Vasyliunas 1968), since it is quasi-Maxwellian at low and thermal energies, while its nonthermal tail decreases as a power-law at high energies, as generally observed in space plasmas; this is in line with the fact that particles of higher

energy have larger free paths and are thus less likely to achieve partial equilibrium. A generating process for such distributions has been suggested recently (Collier 1993). For typical space plasmas,  $\kappa$  generally lies in the range 2–6.

This ‘‘Kappa’’ distribution tends to a Maxwellian for  $\kappa \rightarrow \infty$  since

$$\lim_{\kappa \rightarrow \infty} \left[ 1 + \frac{v^2}{\kappa v_e^2} \right]^{-\kappa-1} = \exp(-v^2/v_e^2). \quad (11)$$

In this limit, all the temperatures  $T_q \rightarrow T_M = m_e v_e^2 / 2k_B$ . For finite  $\kappa$ , however, the temperatures  $T_q$  are different and increase with  $q$ . In particular the traditional temperature is

$$T \equiv T_2 = \frac{m_e v_e^2}{2k_B} \frac{\kappa}{\kappa - 3/2} \quad (12)$$

and the effective temperature  $T_{-2}$  is

$$T_{\text{eff}} \equiv T_{-2} = \frac{m_e v_e^2}{2k_B} \frac{\kappa}{\kappa - 1/2}. \quad (13)$$

The larger  $\kappa$ , the closer the distribution is to a Maxwellian, and the closer the  $T_q$ s are to  $T_M$ .

Substituting (10) into (4), one sees that the distribution at distance  $z$  is still a Kappa function having the same  $\kappa$ . In addition, as a consequence of the form (10), we have

$$f_0[\sqrt{v^2 + V^2}] = \frac{1}{(1 + V^2/\kappa v_e^2)^{\kappa+1}} \times f_0 \left[ \frac{v}{\sqrt{1 + V^2/\kappa v_e^2}} \right].$$

Substituting this relationship into the integral (5) and changing variables to recover  $f_0(v)$  in the integrand, we get

$$M_q(z) = M_q(0) \times [1 + V^2(z)/\kappa v_e^2]^{(q+1)/2-\kappa} \quad (14)$$

(with  $-3 < q < 2\kappa - 2$ , in order that the integrals converge). Since the density is the moment of order  $q = 0$ , this yields

$$\frac{n_e(z)}{n_e(0)} = \left[ 1 + \frac{V^2(z)}{\kappa v_e^2} \right]^{1/2-\kappa}, \quad V^2(z) = 2e|\Phi(z)|/m_e \quad (15)$$

$$\frac{M_q(z)}{M_q(0)} = \left[ \frac{n_e(z)}{n_e(0)} \right]^\alpha \quad (16)$$

with

$$\alpha = 1 - \frac{q/2}{\kappa - 1/2}.$$

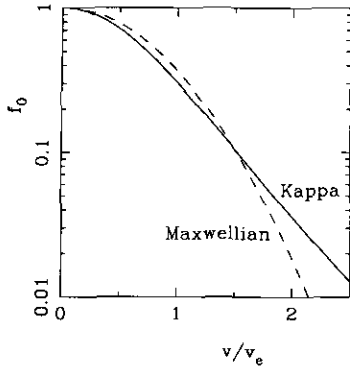


FIG. 3. Kappa distribution defined in Eq. (10) with  $\kappa$  given in (19), compared to its Maxwellian limit (11).

Thus  $M_q/n_e \propto n_e^{-(q/2)/(\kappa-1/2)}$ , and, since  $T_q \propto (M_q/n_e)^{2/q}$ , we deduce

$$T_q \propto n_e^{\gamma-1}, \quad (17)$$

with

$$\gamma = 1 - \frac{1}{\kappa - 1/2}. \quad (18)$$

The  $T_q$ s and  $n_e$  thus follow a polytrope law, which is independent of  $q$ . This generalizes the result of Scudder (1992a) to all the temperatures  $T_q$  and in particular to the temperature  $T_{\text{eff}}$  given by our measurement.

Hence with a Kappa distribution, the density and temperature obey a polytrope law, not only when the temperature is defined from the mean particle energy, but also when it is based on other moments of the distribution, a situation encountered with some measuring techniques.

#### 4.5. Relation between Kappa and the Polytrope Exponent

This simple model can thus explain the polytrope law of index  $\gamma \approx 0.48$  found in Section 3, if the electron velocity distribution can be approximated by a Kappa function of the form (10) with

$$\kappa = \frac{1}{2} + \frac{1}{1-\gamma} \approx 2.4 \pm 0.2. \quad (19)$$

This function is shown in Fig. 3 and compared to its Maxwellian limit given in (11). Both distributions are rather similar for  $v^2 \lesssim \kappa v_e^2$ , i.e., at energies of the order or smaller than  $2-3k_B T_M$ , whereas the Kappa function exhibits a suprathermal tail at higher energies. Note that Eqs. (12)–(13) yield  $T_{\text{eff}}/T = (\kappa - 3/2)/(\kappa - 1/2) \approx 0.5$  with this value of  $\kappa$ . Since measured velocity distributions

are often represented as the superposition of a cold and a hot Maxwellian, we compare in Fig. 4 the above Kappa function with a sum of two Maxwellians having parameters of the order of those inferred from Voyager analyzers in the range of joventric distances explored here (Sittler and Strobel 1987, Bagenal 1994).

In practice, the electron velocity distribution is not *a priori* expected to fit exactly such a Kappa function. Then, one will not find an exact polytrope law, but the density and temperature will still be anticorrelated along field lines and mimic an approximate polytrope with  $\gamma < 1$ . For example, the distribution made of a sum of two Maxwellians also results in a temperature increase with latitude; this can be easily understood: while the temperature of each Maxwellian does not change with  $z$ , the proportion of the hot component increases because it is less confined by the potential. However, with such a cold-plus-hot distribution having parameters of the order of those inferred from Voyager analysers (Fig. 4), the temperature increase is rather small: Eq. (1) shows that a fourfold decrease (for example) in cold density produces an increase in  $T_{\text{eff}}$  by only 5% (instead of the factor of two observed here and explained by the Kappa distribution of Fig. 4). Note also that the magnetic force, which should modify the above result since it does not derive from a conservative potential, is not expected to destroy the anticorrelation between density and temperature so long as the magnetic field variation is small over a characteristic scale length.

## 5. PLASMA DENSITY PROFILE

### 5.1. Density Profile with a Kappa Velocity Distribution

To calculate explicitly the density profile of Eq. (15), we must first calculate the electric potential  $\Phi(z)$ . As usual, one has to calculate the ion density profiles and

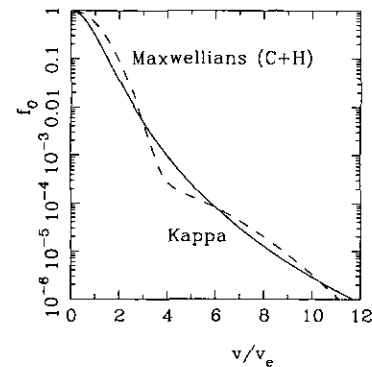


FIG. 4. Kappa distribution defined in Eq. (10) with  $\kappa$  given in (19), compared to a distribution made of the sum of two Maxwellians (C, H) of densities and temperatures such that  $n_H/n_C = 0.02$ ,  $T_H/T_C = 12$  (for this comparison, the cold temperature has been arbitrarily chosen equal to  $T_C = m_e v_e^2 / 1.2 k_B$ ).

then impose charge quasi-neutrality. In the frame of the microscopic formulation considered above, this requires the knowledge of the ion velocity distributions at  $z = 0$ .

Unfortunately, the ion velocity distributions in the torus were not measured aboard Ulysses. They could not be unambiguously determined from Voyager measurements either, because, among other problems, the spectra of individual ion species could not be resolved. Nevertheless, the data indicated that the velocity distributions were not Maxwellian in the corotating frame (Bagenal and Sullivan 1981; Bagenal 1989). Likewise, theoretical models imply highly nonthermal distributions (Richardson and Siscoe 1983, Smith and Strobel 1985). In the spirit of the simple illustrative model considered here, we will assume that there is only one ion species of mass  $m_i$  and charge  $Ze$  and model its non-Maxwellian distribution by a Kappa function having the same  $\kappa$  as the electrons. This is certainly oversimplified, and in particular the values of  $\kappa$  need not be equal for ions and electrons. However, our aim is not to build a detailed empirical model (which would have a large number of unknown parameters since the distributions of individual ion species are poorly known), but rather to explore the consequences of non-Maxwellian distributions. In this context, the Kappa distribution is the simplest choice retaining the basic shape of the measured velocity distributions, which are not too far from Maxwellians at low energies but have power-law suprathermal tails.

So we take for the ion distribution

$$f_0(v) \propto \left[ 1 + \frac{v^2}{\kappa v_i^2} \right]^{-\kappa-1}. \quad (20)$$

The centrifugal force (3) derives from the potential

$$\Phi_c(z) \approx 3m_i\Omega_j^2 z^2/2 \quad (21)$$

(for  $z \ll R$ ). The ions are thus subjected to the total potential ( $\Phi_c + Ze\Phi$ ). As can be verified *a posteriori*, this potential attracts them monotonically (as  $\Phi$  does for the electrons), so that their density profile is given by replacing in the expression (15) of the electron profile “ $e|\Phi|/m_e$ ” by “ $(\Phi_c + Ze\Phi)/m_i$ ”, and  $v_e$  by  $v_i$ . Since charge neutrality requires that  $Zn_i(z) = n_e(z)$ , the electron and ion densities should be proportional to each other, which requires

$$\begin{aligned} \frac{-e\Phi(z)}{m_e v_e^2} &= \frac{\Phi_c(z) + Ze\Phi(z)}{m_i v_i^2} \quad (22) \\ \Rightarrow e\Phi(z) &= \frac{-\Phi_c(z)}{Z + m_i v_i^2 / m_e v_e^2}. \end{aligned}$$

Substituting into (15) with the expression (21) of  $\Phi_c$ , one obtains finally

$$\frac{n_i(z)}{n_i(0)} = \frac{n_e(z)}{n_e(0)} = \left[ 1 + \frac{z^2}{(\kappa - 3/2)H^2} \right]^{1/2-\kappa} \quad (23)$$

$$H^2 = \frac{\kappa}{\kappa - 3/2} \frac{Zm_e v_e^2 + m_i v_i^2}{3m_i \Omega_{\text{spin}}^2}, \quad (24)$$

which is a slightly modified Kappa function. Not unexpectedly, the latitudinal density profile reflects the behavior of the velocity distributions. Note that  $H$  can be expressed as a function of the particle mean random energies at  $z = 0$ , i.e., of the classical temperatures (12) at  $z = 0$ , which we denote by  $T_e(0)$  and  $T_i(0)$  for, respectively, the electrons and the ions; this gives

$$H^2 = \frac{2k_B [ZT_e(0) + T_i(0)]}{3m_i \Omega_{\text{spin}}^2}. \quad (25)$$

## 5.2. Density Profile in a Fluid Approximation

It is important to note that it is not necessary to assume that the velocity distributions are Kappa functions in order to derive such a density profile. One may adopt instead the usual fluid description and solve the corresponding equations along  $\mathbf{B}$ , assuming isotropic pressures and a polytrope law of index  $\gamma < 1$ . These equations read

$$\frac{dp_e}{dz} = -n_e eE \quad (26)$$

$$\frac{dp_i}{dz} = n_i (ZeE + F_c), \quad (27)$$

where  $E = -d\Phi/dz$  is the  $\mathbf{B}$ -aligned electric field. Here, the electron and ion (isotropic) pressures are  $p_{e,i} = n_{e,i} k_B T_{e,i}$ , and we consider the simplest case where electrons and ions obey the same polytrope law  $T_{e,i} \propto n_{e,i}^{\gamma-1}$ . Then  $T_e/T_i = T_e(0)/T_i(0)$ , so that

$$\begin{aligned} \frac{dp_e}{dz} &= \gamma k_B T_e \frac{dn_e}{dz} \quad (28) \\ &= \frac{dp_i}{dz} \times ZT_e(0)/T_i(0). \end{aligned}$$

One gets

$$eE = \frac{-F_c}{Z + T_i(0)/T_e(0)}.$$

Substituting in Eq.(26) and using (28) with  $T_e = T_e(0)[n_e/n_e(0)]^{\gamma-1}$ , one finds

$$\gamma \left[ \frac{n_e(z)}{n_e(0)} \right]^{\gamma-1} \frac{dn_e}{dz} = \frac{nF_c}{k_B[ZT_e(0) + T_i(0)]}.$$

Inserting the expression (3) of  $F_c$  and integrating, one obtains

$$\frac{n_e(z)}{n_e(0)} = \left[ 1 + \frac{z^2}{\gamma H^2(1-\gamma)} \right]^{1/(\gamma-1)} \quad (29)$$

with  $H$  given in (25). This is equivalent to Eq. (23) if  $\gamma$  and  $\kappa$  are related by (18).

Hence a profile of the form (23) can be deduced either from Liouville's theorem, assuming Kappa distribution functions (10) at  $z = 0$ , or from fluid equations, assuming isotropic polytrope laws of index  $\gamma < 1$ , for both electrons and ions. Note that polytropes with exponent  $\gamma > 1$  would give negative densities farther than some finite distance  $z$ , which is unphysical. This is not surprising since, as we have seen, physical velocity distributions generally produce anticorrelated density and temperature along  $z$ , which is not compatible with polytropic exponents  $\gamma > 1$ .

Finally, we note that the classical Gaussian density profile corresponding to statistical equilibrium can be recovered as a particular case of the above derivations, either microscopic (Liouville), by assuming a Maxwellian velocity distribution at  $z = 0$ , or fluid, by taking the limit  $\gamma \rightarrow 1$  in the polytrope law. Indeed, Maxwellians of temperatures  $T_{e,i}(0) = m_{e,i}v_{c,i}^2/2k_B$  are the limits for  $\kappa \rightarrow \infty$  of the Kappa functions (10) and (20) for the electrons and ions, respectively, so that the density profile is obtained by taking the same limit  $\kappa \rightarrow \infty$  in Eq. (23), i.e., referring to (11)

$$\frac{n_e(z)}{n_e(0)} = \exp(-z^2/H^2), \quad (30)$$

with the scale height given in (25). This is just the result of the traditional isothermal torus models in the particular case of one isotropic ion species (Bagenal and Sullivan 1981). Similarly, in the fluid description, this Gaussian profile can be recovered by taking the limit  $\gamma \rightarrow 1$  in Eq. (29).

### 5.3. Comparison with the Measured Density Profile

Let us now compare the measured density profile to the theoretical profile (23), where  $\kappa$  is deduced from the polytrope exponent found in Section 3.

Since the Ulysses trajectory was not exactly normal to equator, we first correct the variation with jovicentric distance. This is done by normalizing the measured den-

sity to the equatorial density at the same jovicentric distance, deduced from Voyager measurements (Sittler and Strobel 1987) by Bagenal (1994) (Fig. 5 of that paper, without current sheet). This assumes that the variation of density with jovicentric distance was similar for Ulysses and Voyager (apart for a constant multiplicative factor  $A$ ) in the small range of distances considered here. Such a procedure may be questionable owing to the differences in epoch and longitude of the spacecraft trajectories; it seems, however, reasonable since it allows to correct completely the small observed latitudinal asymmetry. In order to match our Ulysses results at equator, the densities of the Voyager model must be multiplied by the factor  $A \approx 1.9$ , as in Hoang *et al.* (1993) (i.e., the torus was denser at the time and longitude of the Ulysses traversal, compared to what Voyager measured.)

Our observed profile corrected in this way is plotted in Fig. 5. We have superimposed the Kappa-like profile (23), with  $\kappa$  given in (19), and the scale height

$$H = 0.91R_J.$$

The distance  $z$  (in jovian radii) is counted from the plane of symmetry of the torus as determined from our measurements, which is tilted by  $\alpha \approx 8.3^\circ (\pm 1.6^\circ)$  to the magnetic equator; this value is roughly equal to the nominal  $\approx 7^\circ$  tilt of the centrifugal equator, within the precision of the magnetic field model used. All three parameters ( $H$ ,  $A$ ,  $\alpha$ ) are deduced from a  $\chi^2$  fit involving the data points with

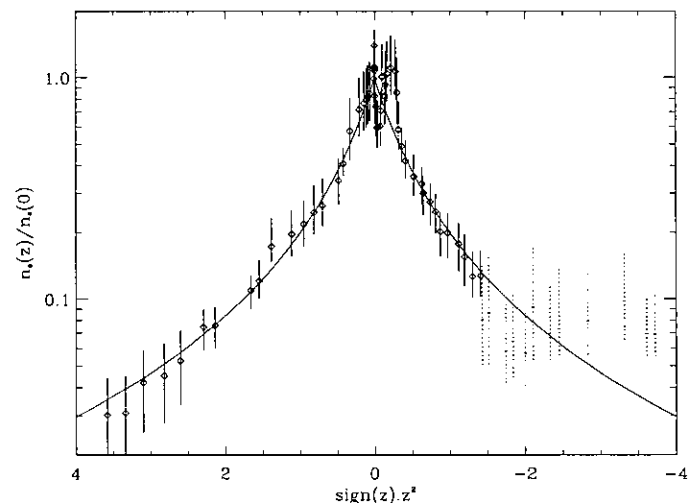


FIG. 5. Theoretical density profile across the Io torus given in Eq. (23) with  $\kappa$  given in (19)—as deduced from the observed polytrope law—and  $H \approx 0.91R_J$ , superimposed to the normalized measured density profile (corrected for the variation with jovicentric distance). The horizontal axis is  $\text{sign}(z) \times z^2$ ,  $z$  being the latitudinal distance in jovian radii. Dotted error bars identify the data for which  $n_e$  and  $T_e$  are not measured independently. The sigma of the fit is 0.04.

solid error bars in Fig. 5. The fit is quite good; the mean-square relative error between the measurements and the model is 0.04.

Substituting in Eq. (25) the Kappa scale height  $H = 0.91R_J$  found above, with the jovian parameters  $R_J \approx 7.14 \times 10^7$  m and  $\Omega_{\text{spin}} \approx 1.76 \times 10^{-4}$  rad/sec, one finds

$$ZT_e(0) + T_i(0) \approx 3 \times 10^4 m_i/m_p$$

( $m_p$  being the proton mass). Assuming an effective ion mass of  $m_i \approx 20 m_p$  at  $R \approx 8R_J$  (Bagenal 1994), this gives  $ZT_e(0) + T_i(0) \approx 6 \times 10^5$  K, which is close to the result found by Hoang *et al.* (1993). It may be noted that in the same range of radial distance, the Voyager measurements imply  $ZT_e \approx 30$  eV and  $T_i \approx 100$  eV (Bagenal 1994). This gives  $ZT_e(0) + T_i(0) \approx 1.5 \times 10^6$  K, which is about 2.5 times larger than our Ulysses determination. Such a difference (if it is not due to the simplifications of our model) is not surprising since (i) with a non-Maxwellian (core) distribution, the Voyager ion (core) temperature, which is determined by assuming the ion (core) distribution to be Maxwellian, is not necessarily equal to the temperature defined from the mean random energy of these particles; (ii) the spacecraft explored different longitude sectors; and (iii) the variability of the torus is known to be significant (see Strobel 1989): for example, the 1981 observations by Morgan (1985) also imply an ion temperature twice smaller than that derived from the Voyager analyzers. One may also note that the radio occultation experiment aboard Ulysses measured a line-of-sight electron content in the torus which similarly suggested an ion temperature twice smaller than the value inferred from Voyager measurements (Bird *et al.* 1993).

We have not included in the fitting the measurements acquired at negative latitudes beyond  $-7^\circ$  (dotted bars in Fig. 4) because in that region the measurements of  $n_e$  and  $T_e$  are not independent. One may note, however, that these points also match the theoretical Kappa-like profile within the error bars, except for the three southernmost points, which do not either follow the polytrope law. Noting that the jovian distance of these points is nearly  $9R_J$ , this might suggest a different origin or behavior of the plasma beyond this distance, where the torus merges into the magnetodisc, and where the influence of the satellite Europa—which orbits Jupiter at  $9.4R_J$ —may be significant (Intriligator and Miller 1982).

It would be interesting to extend the comparison farther from the equator. This is, however, difficult, since Ulysses explored high latitudes in very different longitudes sectors and at very different jovian distances. For an order of magnitude comparison, we note that Ulysses passed at  $z \approx 3R_J$  at the radial distance  $R \approx 6R_J$ , where the Voyager analyzers found an ion temperature  $T_i(0)$

roughly 0.6 times smaller than at  $R \approx 8R_J$ . This yields a scale height roughly  $\sqrt{0.6}$  times smaller than the value above; i.e.  $H \approx 0.7R_J$ . With this parameter, the profile (23) yields  $n_e(3R_J)/n_e(0) \approx 3 \times 10^{-3}$ . Taking  $n_e(0) \approx 2 \times 10^3 \text{ cm}^{-3}$  as determined by Voyager at that radial distance, we obtain  $n_e(3R_J) \approx 6 \text{ cm}^{-3}$ , which is comparable to the values measured aboard Ulysses at this location (Desch *et al.* 1994).

## 6. SUMMARY AND FINAL REMARKS

Our main results are:

1. The electron density and the effective temperature in the outer Io torus are anticorrelated, following an approximate polytrope law of exponent  $\gamma \approx 0.5$ . They were measured *in situ* aboard Ulysses, along a trajectory which crossed the equator basically north-to-south around  $8R_J$  from Jupiter.

2. This can be explained by the filtration of velocities (Scudder 1992a) by the potential which confines the particles to the equator and thus behaves as a high-pass velocity filter for non-Maxwellian distributions. The polytrope exponent  $\gamma \approx 0.5$  is obtained with an electron velocity distribution which can be approximated by a Kappa function with  $\kappa \approx 2.4$ , approaching a Maxwellian at low and thermal energies and joining to a power-law ( $f(v) \propto v^{-7}$ ) at high energies.

3. Our measurements cannot be explained by the usual quasi-thermal model where the electron distribution is made of a Maxwellian plus a Maxwellian tail (isotropic or not). Due to their larger free paths, the ions are even less thermalized than the electrons; this suggests that velocity filtration is at least as effective for the ions, so that they should not be described as fluid species with constant temperatures.

4. Assuming a single isotropic ion species, we have deduced a simple theoretical density profile, whose variation with latitude is Kappa-like instead of the classical (isothermal) Gaussian. This calculated profile fits quite well our measured densities. This profile arises as a direct consequence of Kappa velocity distributions (which have suprathermal tails), just as the Gaussian profile derives from the Maxwellian assumption; it can also be derived from the fluid equations closed with the observed polytrope law, just as the Gaussian can be derived from the fluid equations with a constant temperature. Farther than a scale-height, the Kappa-like profile decreases much more slowly than the Gaussian, since the suprathermal tail is less equatorially confined. Contrary to the traditional density profiles based on Maxwellian distribution functions for all particle species, the Kappa-like density decrease along field lines is power-law farther than a scale height.

The present model is admittedly very crude, since it assumes a single ion species, neglects particle anisotropies and magnetic field variations, considers very simple distribution functions, and ignores temporal and longitudinal variations. It is aimed at explaining the basic trends of our observations, and illustrating in the Io torus the physics implied by the absence of local thermal equilibrium: the temperature(s) increase(s) with latitude, and the density profile is very sensitive to the shape of the particle velocity distributions. It is important to note that our main result (the polytrope relation between  $n_e$  and  $T_e$  and its interpretation) depends only on the electron velocity distribution; it is of course unaffected by the number of ion species, their distributions, and the anisotropies (in the latitude range considered). This leads us to suggest that the traditional assumption of constant temperatures along field lines is expected to be inadequate in the outer torus and should be relaxed in future detailed models.

We have focused here on the smooth variations of the parameters. In the close vicinity of the magnetic equator, we also observed variations over a scale smaller than a few degrees in latitude and/or longitude (Fig. 1), which seem to follow a similar polytropic law. But we have not tried to interpret them, because the instrument temporal resolution (128 sec) makes it difficult to resolve the large gradients involved.

## APPENDIX

Consider a distribution made of a sum of Maxwellians of temperatures  $T_\alpha$  and densities  $n_{\alpha 0}$  at  $z = 0$ . Eq. (4) shows that the distribution at distance  $z$  is a sum of Maxwellians of temperatures  $T_\alpha$  and densities

$$n_\alpha = n_{\alpha 0} e^{-e|\Phi(z)|/k_B T_\alpha}.$$

The temperature of each individual Maxwellian (which, as seen in Section 4, is independent of  $q$  and  $z$ ) is related to its moment  $M_{q\alpha}$  by Eq. (6), i.e.,

$$\frac{k_B T_\alpha}{m_e} = \left[ \frac{M_{q\alpha}}{M_{0\alpha} C_q} \right]^{2/q},$$

where, by definition,  $M_{0\alpha} = n_\alpha$ . The temperature  $T_q$  of the whole distribution at distance  $z$  is obtained by substituting in (6) its moment  $M_q = \sum M_{q\alpha}$  with the above expressions of  $M_{q\alpha}$ .

This gives

$$T_q = \left[ \frac{\sum_\alpha n_\alpha T_\alpha^{q/2}}{\sum_\alpha n_\alpha} \right]^{2/q}.$$

To find the sense of variation of  $T_q$ , we have to calculate the sign of the derivative  $dT_q/dz$ ,

$$\begin{aligned} \text{sgn}(dT_q/dz) = \text{sgn} & \left[ \left( \sum_\alpha n'_\alpha T_\alpha^{q/2} \right) \left( \sum_\alpha n_\alpha \right) \right. \\ & \left. - \left( \sum_\alpha n_\alpha T_\alpha^{q/2} \right) \left( \sum_\alpha n'_\alpha \right) \right], \end{aligned}$$

where

$$n'_\alpha = dn_\alpha/dz = -d|\Phi|/dz \times n_\alpha e/k_B T_\alpha.$$

Thus

$$\begin{aligned} \text{sgn}(dT_q/dz) = \text{sgn}(d|\Phi|/dz) \\ \times \text{sgn} & \left[ \left( \sum_\alpha n_\alpha T_\alpha^{q/2} \right) \left( \sum_\alpha n_\alpha / T_\alpha \right) \right. \\ & \left. - \left( \sum_\alpha n_\alpha T_\alpha^{q/2-1} \right) \left( \sum_\alpha n_\alpha \right) \right]. \end{aligned} \quad (31)$$

The brackets can be rearranged by dropping the terms that cancel out in the summations and symmetrizing over the dummy indices. This gives

$$\begin{aligned} \sum_{\alpha \neq \beta} n_\alpha n_\beta T_\alpha^{q/2} (T_\alpha - T_\beta) / (T_\alpha T_\beta) = \sum_{\alpha > \beta} n_\alpha n_\beta (T_\alpha^{q/2} - T_\beta^{q/2}) \\ (T_\alpha - T_\beta) / (T_\alpha T_\beta), \end{aligned}$$

which is a sum of positive terms, so that the bracket in Eq. (31) is positive. Hence, with a monotonic attractive potential ( $d|\Phi|/dz > 0$ ), the temperatures  $T_q$  all increase with  $z$ . This holds for a velocity distribution which can be modeled by a sum of several Maxwellians (a single Maxwellian giving  $dT_q/dz = 0$ ).

## ACKNOWLEDGMENTS

The Ulysses URAP experiment, whose Principal Investigator is R. G. Stone, is a joint project of NASA/GSFC, Observatoire de Paris, CRPE, and University of Minnesota. The French contribution was mainly financed by the CNES. We are very grateful to the team at the Département de Recherche Spatiale (Observatoire de Paris), who designed, built, and tested the radio astronomy receivers, whose great performances allowed us to obtain these results. We thank our colleagues at GSFC for the successful operation of the experiment during the flyby and their help in the data reduction. We thank D. F. Strobel for his critical reading of an earlier version of this paper and useful suggestions, the referees for their helpful comments, and J. L. Steinberg for his suggestions, which made this paper easier to understand.

## REFERENCES

- BAGENAL, F. 1989. Torus-Magnetosphere coupling. In *Time variable phenomena in the Jovian system* (M. J. S. Belton, R. A. West, and J. Rahe, Eds.), pp. 196-210. NASA SP-494.
- BAGENAL, F. 1994. Empirical model of the Io plasma torus. I. Voyager measurements. *J. Geophys. Res.* **99**, 11043-11062.
- BAGENAL, F., AND J. D. SULLIVAN 1981. Direct plasma measurements in the Io torus and inner magnetosphere of Jupiter. *J. Geophys. Res.* **86**, 8447-8466.
- BALOGH, A., *et al.* 1992. Magnetic field observations during the Ulysses fly-by of Jupiter. *Science* **257**, 1515-1518.
- BARBOSA, D. D., F. V. CORONITI, AND A. EVIATAR 1983. Coulomb thermal properties and stability of the Io plasma torus. *Astrophys. J.* **274**, 429-442.

- BERNSTEIN, I. B. 1958. Waves in a plasma in a magnetic field. *Phys. Rev.* **109**, 10–21.
- BIRD, M. K., S. W. ASMAR, P. EIDENHOFER, O. FUNKE, M. PATZOLD, AND H. VOLLAND 1993. The structure of Jupiter's Io plasma torus inferred from Ulysses radio occultation observations. *Planet. Space Sci.* **41**, 999–1010.
- CHEW, G. F., M. L. GOLDBERGER, AND F. E. LOW. 1956. The Boltzmann equation and the one-fluid hydrodynamic equations in the absence of particle collisions. *Proc. R. Soc. London* **236A**, 112–118.
- CHIU, Y. T., AND M. SCHULZ 1978. Self-consistent particle and parallel electrostatic field distributions in the magnetospheric-ionospheric auroral region. *J. Geophys. Res.* **83**, 629–642.
- COLLIER, M. R. 1993. On generating Kappa-like distribution functions using velocity space Lévy flights. *Geophys. Res. Lett.* **20**, 1531–1534.
- DESCH, M. D., W. M. FARRELL, AND M. L. KAISER 1994. Assymetries in the Io plasma torus. *J. Geophys. Res.* **99**, 17,205–17,210.
- DIVINE, N., AND H. B. GARRETT 1983. Charged particle distributions in Jupiter's magnetosphere. *J. Geophys. Res.* **88**, 6889–6903.
- GLEDHILL, J. A. 1967. Magnetosphere of Jupiter. *Nature* **214**, 155–156.
- HOANG, S., N. MEYER-VERNET, M. MONCUQUET, A. LECACHEUX, AND B. M. PEDERSEN 1993. Electron density and temperature in the Io plasma torus from Ulysses thermal noise measurements. *Planet. Space Sci.* **41**, 1011–1020.
- HUANG, T. S., AND T. J. BIRMINGHAM 1992. The polarization electric field and its effect in an anisotropic rotating plasma. *J. Geophys. Res.* **97**, 1511–1519.
- INTRILIGATOR, D. S., AND W. D. MILLER 1982. First evidence for a Europa plasma torus. *J. Geophys. Res.* **87**, 8081–8090.
- MEYER-VERNET, N. 1993. Aspects of Debye shielding. *Am. J. Phys.* **61**, 249–257.
- MEYER-VERNET, N., AND C. PERCHE 1989. Tool kit for antennae and thermal noise near the plasma frequency. *J. Geophys. Res.* **94**, 2405–2415.
- MEYER-VERNET, N. 1994. On the thermal noise "temperature" in an anisotropic plasma. *Geophys. Res. Lett.* **21**, 397–400.
- MEYER-VERNET, N., S. HOANG, AND M. MONCUQUET 1993. Bernstein waves in the Io plasma torus: A novel kind of electron temperature sensor. *J. Geophys. Res.* **98**, 21163–21176.
- MONCUQUET, M., N. MEYER-VERNET, AND S. HOANG 1995. Dispersion of electrostatic waves in the Io plasma torus and derived electron temperature. Submitted for publication.
- MORGAN, J. S. 1985. Models of the Io torus. *Icarus* **63**, 243–265.
- PRESS, W. H., S. A. TEUKOLSKY, W. T. VETTERLING, AND B. P. FLANNERY 1992. *Numerical Recipes*, 2nd ed., pp. 660–664. Cambridge Univ. Press, Cambridge, UK.
- RICHARDSON, J. D., AND G. L. SISCOE 1983. The non-Maxwellian energy distribution of ions in the warm Io torus. *J. Geophys. Res.* **88**, 8097–8102.
- SCUDDER, J. D. 1992a. On the causes of temperature change in inhomogeneous low-density astrophysical plasmas. *Astrophys. J.* **398**, 299–318.
- SCUDDER, J. D. 1992b. Why all stars should possess circumstellar temperature inversions. *Astrophys. J.* **398**, 319–349.
- SCUDDER, J. D., AND S. OLBERT 1979. A theory of local and global processes which affect solar wind electrons I. The origin of typical 1 AU velocity distribution functions—steady state theory. *J. Geophys. Res.* **84**, 2755–2772.
- SCUDDER, J. D., E. C. SITTLER, JR., AND H. S. BRIDGE 1981. A survey of the plasma electron environment of Jupiter: A view from Voyager. *J. Geophys. Res.* **86**, 8157–8179.
- SISCOE, G. L. 1977. On the equatorial confinement and velocity space distribution of satellite ions in Jupiter's magnetosphere. *J. Geophys. Res.* **82**, 1641–1645.
- SISCOE, G. L., AND D. SUMMERS 1981. Centrifugally driven diffusion of iogenic plasma. *J. Geophys. Res.* **86**, 8471–8479.
- SITTLER, E. C., JR., AND D. F. STROBEL 1987. Io plasma torus electrons: Voyager 1. *J. Geophys. Res.* **92**, 5741–5762.
- SMITH, R. A., AND D. F. STROBEL 1985. Energy partitioning in the Io plasma torus. *J. Geophys. Res.* **90**, 9469–9493.
- SMITH, R. A., F. BAGENAL, A. F. CHENG, AND D. F. STROBEL 1988. On the energy crisis in the Io plasma torus. *Geophys. Res. Lett.* **15**, 545–548.
- SPITZER, L., JR. 1962. *Physics of Fully Ionized Gases*, Interscience, New York.
- STONE, R. G., *et al.* 1992a. The unified radio and plasma wave investigation. *Astron. Astrophys. Suppl. Ser.* **92**, 291–316.
- STONE, R. G., *et al.* 1992b. Ulysses radio and plasma wave observations in the Jupiter environment. *Science* **257**, 1524–1531.
- STROBEL, D. F. 1989. Energetics, luminosity, and spectroscopy of Io's torus. In *Time Variable Phenomena in the Jovian System* (M. J. S. Belton, R. A. West, and J. Rahe, Eds.), pp. 183–195. NASA SP-494.
- VASYLIUNAS, V. M. 1968. A survey of low-energy electrons in the evening sector of the magnetosphere with Ogo 1 and Ogo 3. *J. Geophys. Res.* **73**, 2839–2885.